Case Studies in Thermal Engineering 24 (2021) 100816

Contents lists available at ScienceDirect

Case Studies in Thermal Engineering

journal homepage: http://www.elsevier.com/locate/csite

Investigation of a solar still behaviour using response surface methodology

Oussama Rejeb [a,*], Mohamed S. Yousef [b], Chaouki Ghenai [c,a,**], Hamdy Hassan [d,e], Maamar Bettayeb [g,h]

[a] Sustainable Energy Development Research Group, Research Institute for Science and Engineering (RISE), University of Sharjah, P.O. Box 27272, Sharjah, United Arab Emirates
[b] Mechanical Engineering Department, Benha Faculty of Eng., Benha University, Benha, Egypt
[c] Department of Sustainable and Renewable Energy Engineering, College of Engineering, University of Sharjah, Sharjah, United Arab Emirates
[d] Mech. Eng. Depart. Faculty of Eng., Assiut University, Assiut, Egypt
[e] Energy Resources Eng. Depart., Egypt-Japan University of Science and Technology (E-JUST), Alexandria, Egypt
[g] Department of Electrical Engineering, University of Sharjah, Sharjah, United Arab Emirates
[h] Center of Excellence in Intelligent Engineering Systems (CEIES), King Abdulaziz University, Jeddah, Saudi Arabia

A R T I C L E I N F O

Keywords:
Solar still
Optimization
Response surface methodology (RSM)
Operating parameters
Productivity

A B S T R A C T

This work proposes an innovative statistical model by utilizing the response surface methodology (RSM) method to analyze a batch solar behaviour still. This investigation's main goal is to study the impact of the input factors (solar radiation, ambient temperature, water depth, and thickness of insulation) most influencing water productivity. The polynomial regression model derived from a numerical balance energy model to predict the solar's productivity still is established. The quadratic model is checked by a coefficient of determination (R^2). An excellent fitting is attained between the forecasted results derived from the statistical model and the numerical simulation derived from the heat balance model. The results reveal that the importance of the influence in the order of impact on the amount of distilled water is water depth, solar radiation, ambient temperature, and thickness of insulation. A simple polynomial statistical model is stated in this investigation to determine and maximize the amount of distilled water from solar still based on the four considered input factors.

1. Introduction

In the past few decades, many types of water desalination methods have been used successfully for freshwater production including multiple-effect distillation [1], membrane distillation [2], multistage desalination [3], reverse osmosis [4], and electrodialysis [5]. Most of these techniques are fossil fuel-based desalination methods that result in faster fossil fuel depletion and cause an adverse impact on the environment. Recently, solar water distillation techniques have become more popular due to their promising features of being cost-effective and eco-friendly. Solar stills are simple devices for water purification for which its basis of operation relies on the absorption of solar energy by the salty water, and the water is evaporated and then collected as freshwater after condensation of the

* Corresponding author.
** Corresponding author. Department of Sustainable and Renewable Energy Engineering, College of Engineering, University of Sharjah, Sharjah, United Arab Emirates.
E-mail addresses: oussama.r009@hotmail.fr (O. Rejeb), cghenai@sharjah.ac.ae (C. Ghenai).

https://doi.org/10.1016/j.csite.2020.100816
Received 21 October 2020; Received in revised form 8 December 2020; Accepted 13 December 2020
Available online 2 January 2021

Nomenclature

A	Surface area (m^2)
C	Specific heat ($J\ kg^{-1}\ K^{-1}$)
m	Mass (kg)
k	Thermal conductivity ($W\ m^{-1}\ K$-^{1})
G	Solar irradiation ($W\ m^{-2}$)
h	Heat transfer coefficient ($W\ m^{-2}\ K^{-1}$)
t	Time (s)
L	Thickness (m)

Greek Symbols

α	Absorptivity
ε	Emissivity

Subscripts

sky	Sky
c	Convection
r	Radiation
w	Water
b	Absorber plate
RSM	Response surface methodology
ANOVA	Analysis of variance

vapor [6]. It is commonly recognized that the single slope solar still is the most established one among other designs of solar stills [7]. However, the main shortcoming of this type is its low freshwater productivity which makes its real implementation inapplicable [8].

Several attempts have been undertaken by researchers to improve the thermal performance of solar stills, mostly from three approaches: using improved additive materials, enhancing the structure or adding external auxiliary equipment, such as using porous and wick materials [9,10], using energy-storing materials [11–13], sponge cube [14], black rubber in the still [15], dye [16], capillary film solar still [17]; altering the thickness of insulation [18]; using solar reflectors [19,20], v-corrugated absorbers [21], baffle suspended absorber [22], solar still with pin finned absorber [23]; multi-effect still [24]; pyramid solar still [25]; triple-basin still [26], augmenting the condensation surface area [27–29], partitioning of solar still [30], adding parabolic trough collector to solar still [31–34], using evacuated tube solar collectors [35], thermoelectric modules [36], and hybrid (PV/T) active still [37].

Most of the aforementioned improvement methods entail auxiliary components that increase the capital and operating expenses. By optimization of the operating conditions of the solar still, the thermal efficiency of the solar still can be enhanced without any additional operating expenses [38]. In fact, the productivity of solar still is greatly influenced by environmental and operating conditions such as wind velocity, ambient temperature, solar insolation, inlet water temperature, depth of water, the thickness of insulation, etc … [39]. Solar radiation intensity represents the most important climatic parameter affecting the freshwater productivity of solar stills. Various theoretical and experimental studies have been established to examine the influence of solar insolation on the productivity of solar stills. Morse and Read [40] analytically examined the influence of various parameters comprising solar insolation on the yield of solar still. Their results revealed that the productivity of solar still is significantly affected by the variation of solar intensity values.

The impact of ambient temperature on the performance of solar still is also extensively examined by many researchers [8,41]. It should be pointed out that there are some controversies about the effects of ambient temperature on solar still productivity among different researchers. Garg et al. [42], Copper [43], Malik and Tran [44], and Voropoulos et al. [45] reported that a low ambient temperature or a high wind speed was helpful in improving productivity, while Eibling et al. [46], Hollands [47], Yeh and Chen [48], Hinai et al. [49], and Nafey et al. [50] published a contrary result. The reason of these contradictions may be that a lower ambient temperature or a higher velocity of wind brings greater temperature difference between the brine and the glass cover, as well as a greater heat loss to the surroundings. The former has a positive effect on productivity, while the latter has a negative effect. The depth of water represents one of the most design parameters affecting the performance of solar stills which gained significant attention from many researchers; Tripathi and Tiwari [51] and Phadatare and Verma [52] studied the impact of varying the depth of water on the evaporation rate of passive and active solar stills. Their findings indicated that the freshwater productivity of solar still is inversely proportional to the water brine depth where the freshwater productivity increases as the depth of water decreases. Other parameters such as wind velocity and thickness of insulation have been also comprehensively studied in the literature [53,54].

Response Surface Methodology (RSM), which is a combination of statistical and mathematical approaches, is used for determining optimal conditions for multivariate systems and is recognized as a proficient tool for process optimization [55]. RSM has been widely used to analyze the interactions between different operating parameters and their responses with the objective of optimizing the response. By using this approach, the regression correlation of multiple factors and responses can be estimated. Therefore, RSM has been recently and successfully employed for the performance optimization of engineering systems in different applications [56]. For instance, the thermal performance of direct absorption solar collector (DASC) utilizing three different nanofluids including silver, magnetite and graphite nanoparticles dispersed in water is optimized using RSM by Gorji and Ranjbar [57]. The influence of various operating conditions such as volumetric flow rates, nanoparticle volume fractions and solar intensity on the performance of the proposed system is also considered. The findings indicated that magnetite nanofluid outperforms the other nanofluids in terms of energy and exergy efficiencies. The optimized operating conditions for each nanofluid are also estimated. Najafi et al. [58] optimized the performance of an SI (spark ignition) engine operating with ethanol-gasoline fuel at different blends with the aim of maximizing performance parameters and minimizing emissions using the RSM approach. The optimization results showed that the optimum values were found to be a blend of 90% gasoline (E10) and 10% bioethanol and an engine speed of 3000 rpm. Hatami and Jing [59] performed an optimization study to determine the best wavy profile for the absorber plate of the Direct Absorber Solar Collector with Al_2O_3-water Nanofluid using RSM analysis. The optimization results revealed that the optimal wavy profile includes average wave numbers (λ) and the least possible wave amplitude (Am).

The aforementioned literature survey indicates that most of the preceding studies focused on the parametric investigation of different parameters on the solar still productivity and did not consider any optimization analysis regarding the most parameter affecting the performance of solar still. To the best of the authors' knowledge, no investigation focuses on the development of the regression model to predict the daily productivity outputs for the solar still using RSM, as well as, the study on the influence of the variables most impacting on the daily distilled water productivity related to other parameters has not been studied in the literature. The novelty and authenticity of this work are to establish, for the first time, a polynomial model to forecast the productivity outputs of solar still. The main purpose of this paper is to examine the influences of four input variables most impacting the outputs of the daily productivity, including the weather conditions parameters (solar irradiance, ambient temperature), water depth and thickness of insulation.

The structure of this paper is organized as follows: First, we present the mathematical heat transfer model of the solar still describing the physical phenomenon inside the solar still and the response surface methodology (RSM). Second, a validation of the developed model is performed by comparing the simulated results with the corresponding experimental data to ensure the accuracy of the model. Further, an analysis of variance (ANOVA) and a comparison between the prediction results given from the polynomial model and the numerical results provided by the transient heat numerical model are studied. Finally, the results are analyzed, and a conclusion is presented as a closure section.

2. Mathematical model and numerical solution

2.1. Mathematical thermal model

The solar still consists of the glass cover, brackish water, absorber plate, and insulation. The schematic of our considered solar still is shown in Fig. 1. The transmitted solar radiation enters the solar still collector through the transparent cover, and it is absorbed by the collector plate and then heat is transferred by convection to the saline water. An insulation layer is placed in the back of the solar still to reduce heat loss from the absorber plate. The absorbed plate started to heat, and it transfers its heat by convection to water mass. Under the effect of solar radiation absorbed by the water in the basin and the convection transfer exchange from the plate, the temperature of the water in the basin increases until the evaporation phase and it can be condensing on the inner area of the glazing after releasing its latent heat. It is noteworthy to mention that the analysis is done for batch solar basin (no water is fed to the basin and no water leaves the system except the distilled water production). A multi-physics numerical model based on the coupling of radiative, convective and latent heat, evaporation exchanges within the solar still collector is developed to investigate its behaviour. Considering the sky as a blackbody and assuming constant thermophysical properties of different collector components, and that the absorbed solar flux distribution is homogeneous, the sidewalls are supposed adiabatic, and the condensation is considered only on the glass cover. The

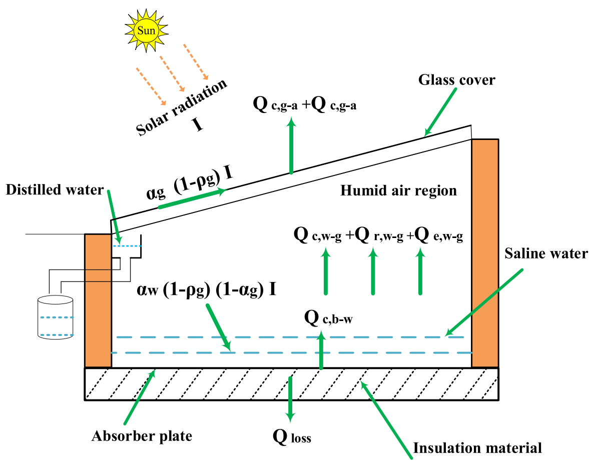

Fig. 1. The heat transfer process in solar still.

lumped energy balance of each component can be written as follows:

2.1.1. Energy balance for glass cover

The energy balance for the glass cover is governed by Ref. [60]:

$$m_c C_c \frac{dT_c}{dt} = A_c(1-\rho_c)\alpha_c I + q_{r,w-c} + q_{ev,w-c} + q_{c,w-c} - q_{r,c-a} - q_{c,c-a} \tag{1}$$

where m_c, $C_c$and $\alpha_c$are the mass, specific heat and absorptivity of the glass cover, respectively. $q_{r,c-a}$ and $q_{c,c-a}$ are the radiation and convective loss from the glazing to the surroundings, respectively. $q_{r,w-c}$ and $q_{c,w-c}$ are the radiation heat exchange between the glazing and the surface water is described as follows. $q_{ev,w-c}$ is the evaporative heat transfer exchange between the glazing and the water surface.

The convective loss from the glazing to the ambient is due to the wind speed and it calculated by the following equation:

$$q_{c,c-a} = \left(6.15V_{wind}^{0.8}\right) A_c\left(T_c - T_{amb}\right) for\ V_{wind} < 5m/s \tag{2}$$

$$q_{c,c-a} = (2.8 + 3\ V_{wind}) A_c\left(T_c - T_{amb}\right) for\ V_{wind} > 5m/s \tag{3}$$

After assuming that the sky is a black body. The infrared radiation exchange between the glazing and the sky can be determined by the following equation:

$$q_{r,c-a} = A_c\ \varepsilon_c\ \sigma\ \left[\left(T_{sky}+273\right)^2\left(T_c+273\right)^2\right]\left(T_c + T_{sky} + 546\right)\left(T_{sky} - T_c\right) \tag{4}$$

where ε_c present the emissivity of glazing.

The sky temperature (T_{sky})can be estimated versus Swinbank's approximation, the sky temperature is related to the ambient temperature, as shown below

$$T_{sky} = 0.0522 \cdot T_{amb}^{1.5} \tag{5}$$

Using the grey surfaces assumption, the radiation heat exchange between the glazing and the surface water is described as follows

$$q_{r,w-c} = \frac{\sigma\left[(T_c+273)^2(T_w+273)^2\right]\left(T_c + T_w + 546\right)}{\frac{1}{\varepsilon_w} + \frac{1}{\varepsilon_c} - 1} A_w\left(T_w - T_c\right) \tag{6}$$

where ε_w present the emissivity of the water surface.

The convective heat transfer exchange between the glazing and the water surface can be estimated by the following equation:

$$q_{c,w-c} = 0.884\left[\left(T_w - T_c\right) + \frac{\left(P_w - P_c\right)(T_w + 273.1)5}{\left(268.9.10^{-3}\right) - P_w}\right]^{0.33} A_w\left(T_w - T_c\right) \tag{7}$$

P_w *and* P_c are, respectively, the partial vapor pressures at water surface temperature and at the inner glazing surface and they are determined by the following equation

$$P_w = \exp\left(25.317 - \frac{5144}{T_w + 273.15}\right) \tag{8}$$

$$P_c = \exp\left(25.317 - \frac{5144}{T_c + 273.15}\right) \tag{9}$$

The evaporative heat transfer exchange between the glazing and the water surface can be determined as follows

$$q_{c,w-c} = \left(16.237.10^{-3}\right)\frac{\left(p_w - p_g\right)}{\left(T_w - T_c\right)}\left[\left(T_w - T_c\right) + \frac{\left(p_w - p_c\right)(T_w)}{268900 - \rho_w}\right]^{0.33} A_w\left(T_w - T_c\right) \tag{10}$$

2.1.2. Energy balance of saline water

The energy balance for the saline water is given by Ref. [60]:

$$m_w C_w \frac{dT_w}{dt} = q_{c,b-w} + A_w(1-\rho_c)(1-\alpha_c)\alpha_w I - q_{ev,w-g} - q_{r,w-g} - q_{c,w-g} \tag{11}$$

where.

m_w C_w and $\alpha_w$are the mass, specific heat, the absorptivity of water in the basin, respectively.

The heat transfer exchange by convection between the surface of the water and the absorber plate can be determined by the following expression

$$q_{c,w-b} = 0.54\left[\left(\frac{k_w.\ \ Ra_w{}^{0.25}}{L_w}\right)A_w(\ \ T_b - \ \ T_w)\ \text{for.}Ra\ 8 * 10^6\right. \tag{12}$$

$$q_{c,w-b} = 0.15\left[\left(\frac{k_w.\ \ Ra_w{}^{0.33}}{L_w}\right)A_w(\ \ T_b - \ \ T_w)\ \text{for.}Ra > 8 * 10^6\right. \tag{13}$$

2.1.3. Energy balance of absorber plate

The energy balance for the absorber plate is given by Ref. [60]:

$$m_b C_b \frac{dT_b}{dt} = A_b(1-\rho_c)(1-\alpha_c)(1-\alpha_w)\alpha_b I - q_{c,b-w} - q_{loss} \tag{14}$$

where.

m_b C_b, ρ_b and $\alpha_b$are the mass, specific heat, density, the absorptivity of the absorber plate, respectively.

q_{loss} is a backward loss to the ambient temperature and it can be determined by the following equation:

$$q_{loss} = \left(\frac{L_b}{k_b} + \frac{L_i}{k_i} + \frac{1}{h_i}\right)^{-1} A_b(\ \ T_b - \ \ T_{amb}) \tag{15}$$

L_b and $k_b$are the thickness and the thermal conductivity of the absorber plate, respectively. L_i and $k_i$are the thickness and the thermal conductivity of insulation, respectively.

2.1.4. Freshwater productivity

The amount of produced freshwater can be expressed by Ref. [60]:

$$m_{ew} = (3600)\frac{A_w\ \ h_{e,w-g}(\ \ T_w - T_g)}{\lambda_{fg}} \tag{16}$$

where $\lambda_{fg}$is the latent heat of vaporization and it is given by Ref. [60]:

$$\lambda_{fg} = 3.1615(10^6 - 761.6T_{wg})T_{wg} > 70 \tag{17}$$

$$\lambda_{fg} = 2.4935\ \begin{pmatrix} n10^6 - 947.79 \times T_{wg} + 0.13132 \times T_{wg}^2 \\ n - 0.0047974 \times T_{wg}^3 \end{pmatrix}, \quad T_{wg} < 70 \tag{18}$$

where,

$$T_{wg} = \frac{(\ \ T_w + T_g)}{2} \tag{19}$$

2.2. Validation of the numerical model

The fourth-order Runge-Kutta method (ode45) is used to solve the differential equations system governing the transient thermal behaviour (Eq. (1), (11) and (14)). The Runge-Kutta method is characterized by its precision and stability to solve the ordinary differential equations (ODE). In order to assess the accuracy of the established model, the numerical results of solar still temperatures and water productivity are compared with the corresponding experimental data of Yousef and Hassan [11]. The root mean square percentage deviation (RMSD) is used as a useful measure of data agreement between numerical and experimental findings which can be expressed by Ref. [60]:

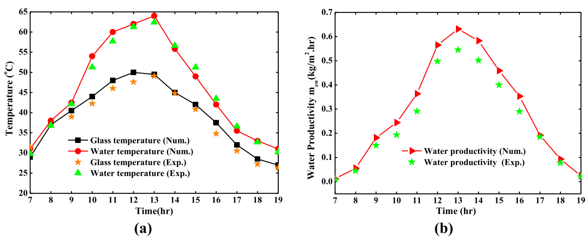

Fig. 2. Validation of simulated results of (a) glass and water temperatures (b) water productivity with experimental data of [11].

$$RMS = \frac{\sqrt{\frac{\sum\left(100*\left(X_{exp,i}-X_{num,i}\right)\right)}{\left(X_{exp,i}\right)^2}}}{n_{exp}} \tag{20}$$

where $X_{exp,i}$and $X_{num,i}$ are the experimental and numerical values, respectively.

Fig. 2 represents the comparison of the hourly variation of simulation results of glass and saline water temperatures with the corresponding experimental data provided by Yousef and Hassan [11]. It is obvious from Fig. 1 that the glass cover and saline water temperatures increase gradually with time until they reach a maximum value at about 13:00 p.m. (solar noon); thereafter they start to reduce with increasing time. Also, it can be noticed that there is a good correspondence between the simulation results and the experimental data. For the temperatures of the glass cover and saline water, the estimated RMSD is 2.57% and 2.15%, respectively. To further evaluate the accuracy of the developed model, the hourly variations of the simulated hourly productivity are compared with the experimental data given by Yousef and Hassan [11] as depicted also in Fig. 2. It can be seen that the distillate yield steadily increases and reaches a maximum value at 13:00 p.m. where the solar radiation reaches its maximum value. Then, it decreases gradually till the end of the measuring time. It is observed that the simulation results for the amount of collected distilled water are in close agreement with the experimental data and its RMSD is about 3.13%.

3. Response surface methodology (RSM)

Response Surface Methodology (RSM) is a combination of mathematical and statistical methods, which is helpful to develop, optimize and improve processes. One of the helpful features of RSM is to develop an accurate model between the response and independent variables using the analysis of variance method (ANOVA). The quadratic polynomial regression model is used and is expressed by the following equation:

$$y = \beta_0 + \sum_{i-1}^{n} \beta_i x_i + \sum_{i=1}^{n} \beta_{ii} {x_i}^2 + \sum_{i=1}^{n-1} \sum_{j-i+1}^{n} \beta_{ij} x_i x_j \tag{21}$$

The correctness of the quadratic polynomial regression model is verified by the adjusted multiple determination coefficient and the coefficient of multiple determination.

The multiple determination coefficient (R^2) can be determined as follows:

$$R^2 = 1 - \frac{SS_E}{SS_T} \tag{22}$$

where.

SS_T and SS_E are the sum of the squares and the sum of the residuals, respectively and they can be determined by the following equation

$$SS_T = \sum_{i=1}^{n} (y_i)^2 - \frac{\sum_{i=1}^{n} (y_i)^2}{n} \tag{23}$$

$$SS_T = \sum_{i=1}^{n} (y_i - \widetilde{y}_i)^2 \tag{24}$$

y_i and $\widetilde{y}_i$ are the observations and fitted values, respectively. n designates the number of observations.

The adjusted multiple determination-adjusted coefficients can be estimated by the following equation:

$$R_{adj}{}^2 = 1 - \left(1 - R^2\right) \frac{n-1}{n-P} \tag{25}$$

P designates the regression coefficients number.

Table 1
Range of selected input variables.

Variables	Levels		
	−1	0	1
A: Solar radiation (W/m^2)	300	600	900
B: Ambient temperature (°C)	25	35	45
C:Water depth (m)	0.01	0.03	0.05
D:Thickness insulation (m)	0.01	0.04	0.07

3.1. Application of response surface methodology

In this paper, impact in order of importance of four factors, i.e., the solar radiation, ambient temperature, water depth and the thickness of insulation, on the efficiency of solar still is studied. As presented in Tables 1 and 2, four factors are varied over three levels (low, middle and higher). A central composite design (CCD), with face central, is chosen. To determine the number of points needed for the four studied parameters, the following correlation is used:

$$N = 2^k + 2k + n_c = 2^4 + 2.4 + 6 = 30 \tag{26}$$

where N indicates the runs number, k designates the factors number,n_c denotes the number of replications at the central design point.

3.1.1. Analysis of variance (ANOVA)

To evaluate the adequacy of the formulated polynomial model, an analysis of variance (ANOVA) is performed (see Table 3). A 112.55 value of (F-test) and (<0.0001) p-value are obtained, which means the signification of the proposed model. The p-value is represented as the choice to the elimination points to give the least level of importance at which the null hypothesis would be rejected. In addition, the influence of linear variable (A: solar radiation, B: ambient temperature, and C: water depth), interactions of factors (AC: solar radiation and water depth) and quadratic terms (C^2: water depth^2) signify the most significant terms. As seen in Fig. 3, the comparison between the freshwater productivity given by our established heat transfer model by implemented in MATLAB and the forecasting data by the regression polynomial model verifies the adjacency of predicted data to actual data. The values of R-squared and Adjusted R-squared are 0.9906 and 0.9818, respectively, reflecting a fine adjustment between the prediction results given from the polynomial model and the numerical results provided by the heat transfer numerical model described in Section 2.1. Signal to noise rate for the solar still efficiency is 36.672, (While values higher than four are acceptable for the satisfactory precision), which confirms that the regression model can be used to examine the performance of our solar still collector with high sufficiency and reliability.

3.2. Model estimation

The following correlation expresses the polynomial model for the freshwater productivity of solar still related to individual, quadratic, and interaction of variables.

Table 2
Actual values of independent variables along with their responses of daily productivity (kg/m^2) output.

Run	Factor 1	Factor 2	Factor 3	Factor 4	Response 1
	A:Solar radiation (W/m^2)	B:Ambient Temperature (°C)	C:Water Depth (m)	D:thickness of the insulation (m)	Daily productivity
1	600	35	0.05	0.04	0.38761
2	600	25	0.03	0.04	0.45108
3	600	35	0.03	0.04	0.62997
4	300	45	0.01	0.07	0.84856
5	600	35	0.03	0.04	0.62997
6	600	35	0.03	0.04	0.62997
7	600	35	0.03	0.07	0.63244
8	900	45	0.01	0.07	2.53573
9	900	45	0.05	0.01	0.76763
10	900	25	0.01	0.07	2.49854
11	300	35	0.03	0.04	0.32334
12	900	45	0.05	0.07	0.77491
13	300	45	0.01	0.01	0.83017
14	900	25	0.05	0.07	0.4045
15	300	25	0.01	0.01	0.50184
16	600	35	0.01	0.04	1.63863
17	600	45	0.03	0.04	0.82953
18	300	25	0.05	0.07	0.15661
19	900	25	0.05	0.01	0.40005
20	900	45	0.01	0.01	2.48021
21	300	45	0.05	0.07	0.33008
22	600	35	0.03	0.01	0.62413
23	600	35	0.03	0.04	0.62997
24	300	25	0.01	0.07	0.51539
25	300	25	0.05	0.01	0.15523
26	900	25	0.01	0.01	2.42855
27	300	45	0.05	0.01	0.32757
28	600	35	0.03	0.04	0.62997
29	900	35	0.03	0.04	1.02184
30	600	35	0.03	0.04	0.62997

Table 3
Analysis of variance for daily productivity (kg/m^2) for solar still.

Source	Sum of Squares	df	Mean Square	F-value	p-value	
Model	14.42	14	1.03	112.54	<0.0001	significant
A-Solar radiation	4.83	1	4.83	527.80	<0.0001	
B-Ambient Temperature	0.2720	1	0.2720	29.73	<0.0001	
C-Water Depth	6.21	1	6.21	678.85	<0.0001	
D-thickness of the insulation	0.0018	1	0.0018	0.1998	0.6613	
AB	0.0020	1	0.0020	0.2225	0.6439	
AC	2.15	1	2.15	235.34	<0.0001	
AD	0.0006	1	0.0006	0.0703	0.7946	
BC	0.0069	1	0.0069	0.7596	0.3972	
BD	2.009E-06	1	2.009E-06	0.0002	0.9884	
CD	0.0013	1	0.0013	0.1374	0.7160	
A^2	0.0015	1	0.0015	0.1600	0.6948	
B^2	0.0002	1	0.0002	0.0206	0.8879	
C^2	0.3438	1	0.3438	37.58	<0.0001	
D^2	0.0011	1	0.0011	0.1195	0.7344	
Residual	0.1372	15	0.0091			
Lack of Fit	0.1372	10	0.0137			
Pure Error	0.0000	5	0.0000			
Cor Total	14.55	29				

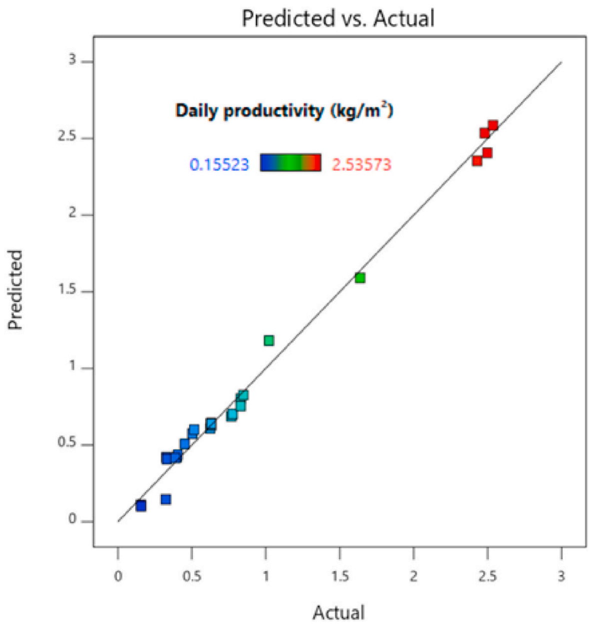

Fig. 3. Comparison between the predicted results provided by RSM against the simulation of the daily productivity of solar still.

$$\begin{aligned} \text{Daily productivity}\left(\frac{\text{kg}}{\text{m}^2}\right) = & -0.257742 + \left(0.003347 * A\right) + \left(0.00017432 * B\right) - \left(50.38702 * C\right) + \left(2.22359 * D\right) \\ & - \left(3.75979.\left(10^{-6}\right) * \left(A * B\right)\right) - \left(0.06114 * A * C\right) + \left(0.000704 * A * D\right) + \left(0.104203 * B * C\right) \\ & - \left(0.001181 * B * D\right) - \left(14.77396 * C * D\right) + \left(2.64068.\left(10^{-7}\right) * A^2\right) - \left(0.000085 * B^2\right) \\ & + \left(910.74035 * C^2\right) - \left(22.82096 * D^2\right) \end{aligned} \tag{27}$$

4. Results and discussion

4.1. Main effects of parameters on the response

In order to make an evaluation of the responses of the examined parameters at a particular point in the considered design space, the perturbation graph is plotted. In this graph, the response is presented by changing only one parameter over its span while keeping all the other parameters fixed. The perturbation graph showing the variation of solar radiation, ambient temperature, water depth, and the thickness of insulation on the freshwater productivity of solar still is depicted in Fig. 4. It is observed that as the solar intensity, ambient temperature and thickness of insulation values increases, the rates of freshwater productivity also increases. On the contrary, Fig. 4 also indicates that increasing the water depth negatively affects the water productivity. Such findings are consistent with Eq. (27) where solar intensity, ambient temperature, and thickness of insulation have a positive coefficient whereas the water depth has a negative coefficient. Upon closer inspection of the parameters coefficients in Eq. (27), it was found that the most significance of each parameter on distilled water produced is in order: water depth > solar radiation > ambient temperature > thickness of insulation.

5.2. Binary effects of parameters on the response

5.2.1. Effect of solar radiation and ambient temperature on the performance of solar still

The variation of freshwater productivity of solar still versus the solar radiation and the ambient temperature is presented in Fig. 5. The solar radiation is varied from 300 W/m^2 to 900 W/m^2, and the ambient temperature is changed from 25 °C to 45 °C. The other parameters, such as water depth and the thickness of insulation, are fixed at 0.03 m and 0.04 m, respectively. It can be depicted from Fig. 5 that solar radiation represents a significant impact on influencing the solar still performance compared to the ambient temperature. At the fixed value of ambient temperature (45 °C), the solar still productivity increases from 0.44 kg/m^2 to 1.303 kg/m^2 as the solar radiation rises from 300 to 900 W/m^2. The increased solar radiation raises the operating temperature of water in the basin. The rise in the temperature of the water temperature has a positive impact on the evaporation rate and therefore, the increase in distillate water productivity. Besides, for 900 W/m^2 value of solar radiation, when the ambient temperature increases from 25 °C to 45 °C, an augmentation in distillate water productivity rate from 0.755 kg/m^2 to 1.303 kg/m^2 is achieved. On the other hand, the increase of the ambient temperature results in the decrease of solar collector heat losses and therefore, the gradient temperature between condensing glass cover and saline water in the basin increases, thus enhancing the distilled water productivity.

5.2.2. Effect of water depth and thickness of insulation on the performance of solar still

The water depth is changed from 0.01 m to 0.03 m, and the thickness of the insulation is changed from 0.01 m to 0.07 m. The other parameters, such as solar radiation and the ambient temperature, are fixed at 600 W/m^2 and 35 °C, respectively. The productivity of solar still versus the water depth and thickness of insulation is presented in Fig. 6. However, from Fig. 6, we can see that the water depth represents a significant impact on influencing the solar still efficiency compared to the thickness of insulation. At the fixed value of the thickness of insulation (0.07 m), the solar still productivity decreases from 1.65 kg/m^2 to 0.388 kg/m^2 as the water depth rises from 0.01 m to 0.05 m. The increase of water volume and the water volumetric heat capacity in the basin results in a reduction in saline

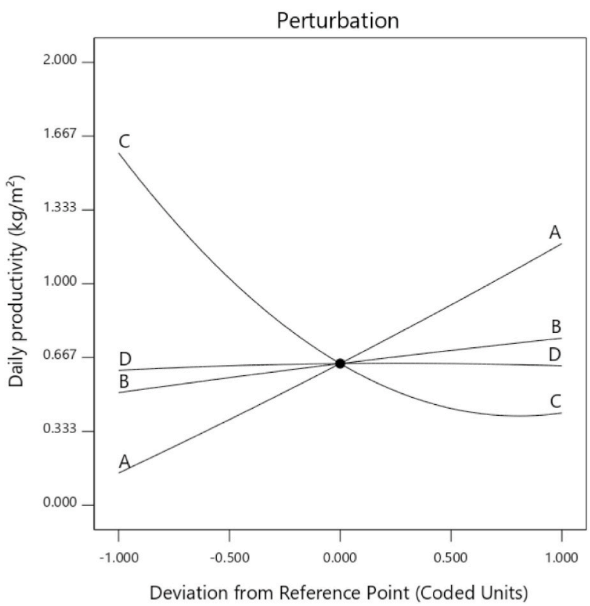

Fig. 4. Perturbation plot for daily productivity (for A: solar radiation, B: ambient temperature, C: water depth, D: Thickness of insulation).

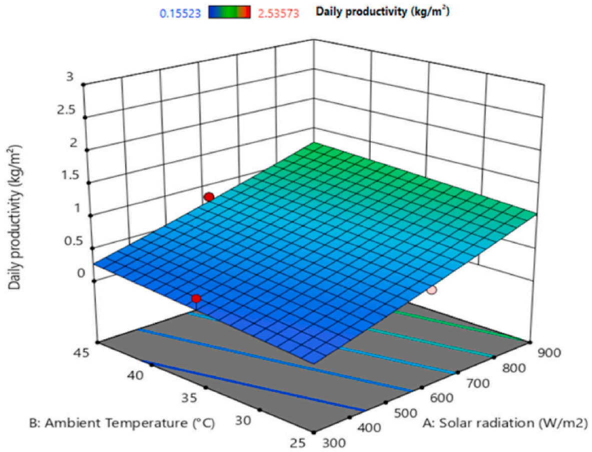

Fig. 5. 3D response surface plot illustrating interaction effects of solar radiation and ambient temperature on the daily productivity of the solar still.

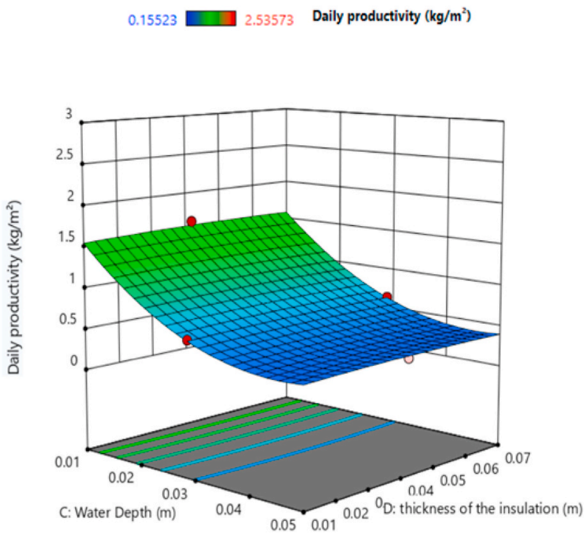

Fig. 6. 3D response surface plot illustrating interaction effects water Depth and thickness of insulation on the daily productivity of the solar still.

water temperature. Accordingly, lower temperature difference between the glass cover and water temperatures is achieved, resulting in a reduction in convective heat transfer coefficient rates between glass cover and saline water and thus low freshwater productivity is obtained. Consequently, a reduced water depth leads to an enhancement in evaporation rates of water for constant solar energy input. Besides, for 0.01 m value of water depth, when the thickness of insulation increases from 0.01 m to 0.05 m, an augmentation in distillate water productivity rate from 1.61 kg/m^2 to 1.62 kg/m^2 is achieved. On the other hand, the increases of the thickness of insulation results in the decrease of the back heat losses and therefore, an increase in temperature of the water, thus enhancing the distilled water productivity.

5. Conclusions

In this investigation, a numerical work is conducted to assess the influence of four factors, i.e., solar radiation, ambient temperature, water depth and thickness of insulation on the daily productivity outputs for the solar still.

Based on the thermal transient model, a polynomial statistical model was presented to predict the solar still's daily productivity outputs. The interactions between the examined factors and their combined influences on the daily distilled water productivity are performed utilizing a statistical RSM model.

The Analysis of Variance is conducted to obtain the significance of the established regression models. The main conclusions are:

- The values of R-squared and Adjusted R-squared are 0.9906 and 0.9818. A good adjustment between the prediction results given from the polynomial model and the numerical results provided by the transient heat numerical model.

- The impacts of the influence in the order of importance on daily distilled water productivity are respectively water depth, solar radiation, ambient temperature, and thickness of insulation.
- The simple polynomial statistical model can be applied to calculate and maximize the daily productivity from solar still based on the four examined input variables.

Future work will involve the influences of dust, Nanoparticle-Enhanced Phase Change Materials (NEPCM), and various absorber geometries on the productivity of the solar still.

Author statement

Oussama Rejeb: Conceptualization, Methodology, Software, Validation, Formal analysis, Investigation, Writing - original draft, Writing - review & editing.
Mohamed S. Yousef: Conceptualization, Methodology, Software, Validation, Formal analysis, Investigation, Writing - original draft, Writing - review & editing.
Chaouki Ghenai: Conceptualization, Methodology, Software, Validation, Formal analysis, Investigation, Writing - original draft, Writing - review & editing.
Hamdy Hassan: Conceptualization, Methodology, Software, Validation, Formal analysis, Investigation, Writing - original draft, Writing - review & editing.
Maamar Bettayeb: Conceptualization, Methodology, Software, Validation, Formal analysis, Investigation, Writing - original draft, Writing - review & editing.

Declaration of competing interest

The authors declare that they have no known competing financial interests or personal relationships that could have appeared to influence the work reported in this paper.

Acknowledgements

The authors gratefully acknowledge the financial support from the Sustainable Energy and Power Systems Research Center, Research Institute For Sciences and Engineering, University of Sharjah, Sharjah, United Arab Emirates.

References

[1] D.C. Alarcón-padilla, L. García-rodríguez, J. Blanco-gálvez, Design recommendations for a multi-effect distillation plant connected to a double-effect absorption heat pump : a solar desalination case study, DES 262 (2010) 11–14, https://doi.org/10.1016/j.desal.2010.04.064.
[2] J. Liu, Q. Wang, H. Shan, H. Guo, B. Li, Surface hydrophobicity based heat and mass transfer mechanism in membrane distillation, J. Membr. Sci. (2019), https://doi.org/10.1016/j.memsci.2019.01.057.
[3] C. Hanshik, H. Jeong, K. Jeong, S. Choi, Improved productivity of the MSF (multi-stage fl ashing) desalination plant by increasing the TBT (top brine temperature), Energy 107 (2016) 683–692, https://doi.org/10.1016/j.energy.2016.04.028.
[4] M. Qasim, M. Badrelzaman, N.N. Darwish, N.A. Darwish, Reverse Osmosis Desalination : A State-Of-The-Art Review, vol. 459, 2019, pp. 59–104, https://doi.org/10.1016/j.desal.2019.02.008.
[5] L. Lauer, L. Marder, T. Benvenuti, A. Moura, Journal of Environmental Chemical Engineering Electrodialysis applied to the treatment of an university sewage for water recovery, J. Environ. Chem. Eng. 7 (2019), 102982, https://doi.org/10.1016/j.jece.2019.102982.
[6] D.B. Singh, Improving the performance of single slope solar still by including N identical PVT collectors, Appl. Therm. Eng. 131 (2018) 167–179, https://doi.org/10.1016/j.applthermaleng.2017.11.146.
[7] K. Selvaraj, A. Natarajan, Factors influencing the performance and productivity of solar stills - a review, Desalination (2017), 0–1, https://doi.org/10.1016/j.desal.2017.09.031.
[8] M. Shadi, S. Abujazar, S. Fatihah, A.R. Rakmi, M.Z. Shahrom, The effects of design parameters on productivity performance of a solar still for seawater desalination : a review, DES 385 (2016) 178–193, https://doi.org/10.1016/j.desal.2016.02.025.
[9] M.S. Yousef, H. Hassan, H. Sekiguchi, Energy, exergy, economic and enviroeconomic (4E) analyses of solar distillation system using different absorbing materials, Appl. Therm. Eng. (2019), https://doi.org/10.1016/j.applthermaleng.2019.01.005.
[10] A.R.A. Elbar, M.S. Yousef, H. Hassan, Energy, exergy, exergoeconomic and enviroeconomic (4E) evaluation of a new integration of solar still with photovoltaic panel, J. Clean. Prod. (2019), https://doi.org/10.1016/j.jclepro.2019.06.111.
[11] M.S. Yousef, H. Hassan, An experimental work on the performance of single slope solar still incorporated with latent heat storage system in hot climate conditions, J. Clean. Prod. (2019), https://doi.org/10.1016/j.jclepro.2018.11.120.
[12] M.S. Yousef, H. Hassan, Energetic and exergetic performance assessment of the inclusion of phase change materials (PCM) in a solar distillation system, Energy Convers. Manag. (2019), https://doi.org/10.1016/j.enconman.2018.10.078.
[13] M.S. Yousef, H. Hassan, Energy payback time, exergoeconomic and enviroeconomic analyses of using thermal energy storage system with a solar desalination system: an experimental study, J. Clean. Prod. 270 (2020), 122082, https://doi.org/10.1016/j.jclepro.2020.122082.
[14] R.L. Narayana, V.R. Raju, Experimental investigation OF a passive solar still with and without tetrahedral sponge IN basin, Int. J. Ambient Energy (2017) 1–16, https://doi.org/10.1080/01430750.2017.1392349.
[15] A.S. Nafey, M. Abdelkader, A. Abdelmotalip, A.A. Mabrouk, Solar still productivity enhancement, Energy Convers. Manag. 42 (2001) 1401–1408, https://doi.org/10.1016/S0196-8904(00)00107-2.
[16] B.A.K. Abu-hijleh, Effect of Water Emissivity on Solar Still Efficiency, 2010, https://doi.org/10.1080/0142591031000148605.
[17] M. Zerrouki, N. Settou, Y. Marif, M. Mustapha, Simulation study of a capillary film solar still coupled with a conventional solar still in south Algeria, Energy Convers. Manag. 85 (2014) 112–119, https://doi.org/10.1016/j.enconman.2014.05.062.
[18] A.G.M. Ibrahim, I. Dincer, A solar desalination system: exergetic performance assessment, Energy Convers. Manag. 101 (2015) 379–392, https://doi.org/10.1016/j.enconman.2015.05.060.

[19] Z.M. Omara, A.E. Kabeel, M.M. Younes, Enhancing the stepped solar still performance using internal and external reflectors, Energy Convers. Manag. 78 (2014) 876–881, https://doi.org/10.1016/j.enconman.2013.07.092.
[20] Z.M. Omara, A.E. Kabeel, A.S. Abdullah, F.A. Essa, Experimental investigation of corrugated absorber solar still with wick and reflectors, Desalination 381 (2016) 111–116, https://doi.org/10.1016/j.desal.2015.12.001.
[21] S.M. Shalaby, E. El-Bialy, A.A. El-Sebaii, An experimental investigation of a v-corrugated absorber single-basin solar still using PCM, Desalination 398 (2016) 247–255, https://doi.org/10.1016/j.desal.2016.07.042.
[22] E. El-Bialy, A.A. El-Sebaii, S. Aboul-Enein, Single Basin Solar Still with Baffle Suspended Absorber, vol. 41, 2000, pp. 661–675.
[23] M.S. Yousef, H. Hassan, Assessment of different passive solar stills via exergoeconomic, exergoenvironmental, and exergoenviroeconomic approaches: a comparative study, Sol. Energy (2019), https://doi.org/10.1016/j.solener.2019.02.042.
[24] K.S. Reddy, K.R. Kumar, T.S.O. Donovan, T.K. Mallick, Performance analysis of an evacuated multi-stage solar water desalination system, DES 288 (2012) 80–92, https://doi.org/10.1016/j.desal.2011.12.016.
[25] N. Abdelal, Y. Taamneh, Enhancement of pyramid solar still productivity using absorber plates made of carbon fi ber/CNT-modi fi ed epoxy composites, Desalination 419 (2017) 117–124, https://doi.org/10.1016/j.desal.2017.06.012.
[26] A.A. El-Sebaii, Thermal Performance of a Triple-Basin Solar Still, vol. 174, 2005, pp. 23–37, https://doi.org/10.1016/j.desal.2004.08.038.
[27] H. Hassan, Energy , exergy , environmental , and economic analysis of natural and forced cooling of solar still with porous media, Environ. Sci. Pollut. Res. 27 (2020) 38221–38240, https://doi.org/10.1007/s11356-020-09995-4.
[28] H. Hassan, M.S. Yousef, M. Fathy, M.S. Ahmed, Impact of condenser heat transfer on energy and exergy performance of active single slope solar still under hot climate conditions, Sol. Energy 204 (2020) 79–89, https://doi.org/10.1016/j.solener.2020.04.026.
[29] S. Abo-Elfadl, M.S. Yousef, H. Hassan, Energy, exergy, economic and environmental assessment of using Different passive condenser designs of solar distiller, Process Saf. Environ. Protect. 148 (2020) 302–312, https://doi.org/10.1016/j.psep.2020.10.022.
[30] S. Rashidi, J. Abolfazli, N. Rahbar, Partitioning of solar still for performance recovery : experimental and numerical investigations with cost analysis, Sol. Energy 153 (2017) 41–50, https://doi.org/10.1016/j.solener.2017.05.041.
[31] H. Hassan, M.S. Yousef, Productivity, exergy, exergoeconomic, and enviroeconomic assessment of hybrid solar distiller using direct salty water heating, Environ. Sci. Pollut. Res. (2020), https://doi.org/10.1007/s11356-020-10803-2.
[32] H. Hassan, M.S. Yousef, An assessment of energy, exergy and CO2 emissions of a solar desalination system under hot climate conditions, Process Saf. Environ. Protect. 145 (2021) 157–171, https://doi.org/10.1016/j.psep.2020.07.043.
[33] H. Hassan, M.S. Ahmed, M. Fathy, M.S. Yousef, Impact of salty water medium and condenser on the performance of single acting solar still incorporated with parabolic trough collector, Desalination (2020), 114324, https://doi.org/10.1016/j.desal.2020.114324.
[34] H. Hassan, M.S. Yousef, M. Fathy, M.S. Ahmed, Assessment of parabolic trough solar collector assisted solar still at various saline water mediums via energy, exergy, exergoeconomic, and enviroeconomic approaches, Renew. Energy (2020), https://doi.org/10.1016/j.renene.2020.03.126.
[35] M.B. Shafii, M. Shahmohamadi, M. Faegh, H. Sadrhosseini, Examination of a novel solar still equipped with evacuated tube collectors and thermoelectric modules, Desalination 382 (2016) 21–27, https://doi.org/10.1016/j.desal.2015.12.019.
[36] S. Nazari, H. Safarzadeh, M. Bahiraei, Performance improvement of a single slope solar still by employing thermoelectric cooling channel and copper oxide nanofluid: an experimental study, J. Clean. Prod. (2018), https://doi.org/10.1016/j.jclepro.2018.10.194.
[37] P. Pounraj, D.P. Winston, A.E. Kabeel, B.P. Kumar, A.M. Manokar, R. Sathyamurthy, S.C. Christabel, Experimental investigation on Peltier based hybrid PV/T active solar still for enhancing the overall performance, Energy Convers. Manag. 168 (2018) 371–381, https://doi.org/10.1016/j.enconman.2018.05.011.
[38] H. Tanaka, Parametric investigation of a vertical multiple-effect diffusion solar still coupled with a tilted wick still, Desalination 408 (2017) 119–126, https://doi.org/10.1016/j.desal.2017.01.019.
[39] P. Durkaieswaran, K.K. Murugavel, Various special designs of single basin passive solar still – a review, Renew. Sustain. Energy Rev. 49 (2015) 1048–1060, https://doi.org/10.1016/j.rser.2015.04.111.
[40] R.N.R.W.R.W. Morse, A Rational Basis for the Engineering Development of a Solar Still, vol. 12, 1968, pp. 5–17.
[41] A.F. Muftah, M.A. Alghoul, A. Fudholi, M.M. Abdul-Majeed, K. Sopian, Factors affecting basin type solar still productivity: a detailed review, Renew. Sustain. Energy Rev. 32 (2014) 430–447, https://doi.org/10.1016/j.rser.2013.12.052.
[42] M.H. Garg Hp, Effect of Climatic, Operational and Design Parameters on the Year Round Performance of Single-Sloped and Double-Sloped Solar Still under Indian Arid Zone Conditions, vol. 30328, 1975, pp. 1–17.
[43] P.I. Cooper, The maximum efficiency of single-effect solar stills, Sol. Energy 15 (1973) 205–217, https://doi.org/10.1016/0038-092X(73)90085-6.
[44] M.A.S. Malik, Vi Van Tran, A simplified mathematical model for predicting the nocturnal output of a solar still, Sol. Energy 14 (1973) 371–385, https://doi.org/10.1016/0038-092X(73)90015-7.
[45] K. Voropoulos, E. Mathioulakis, V. Belessiotis, Experimental investigation of the behavior of a solar still coupled with hot water storage tank, Desalination 156 (2003) 315–322, https://doi.org/10.1016/S0011-9164(03)00362-X.
[46] J.A. Eibling, S.G. Talbert, G.O.G. Löf, Solar stills for community use-digest of technology, Sol. Energy 13 (1971) 263–276, https://doi.org/10.1016/0038-092X(71)90007-7.
[47] K.G.T. Hollands, The regeneration of lithium chloride brine in a solar still for use in solar air conditioning, Sol. Energy 7 (1963) 39–43, https://doi.org/10.1016/0038-092X(63)90003-3.
[48] H.M. Yeh, L.C. Chen, The effects of climatic, design and operational parameters on the performance of wick-type solar distillers, Energy Convers. Manag. 26 (1986) 175–180, https://doi.org/10.1016/0196-8904(86)90052-X.
[49] B.A.H. Al-Hinai, M.S. Al-Nassri, Jubran, Effect of Climatic , Design and Operational Parameters on the Yield of a Simple Solar Still, vol. 43, 2002, pp. 1639–1650.
[50] A.S. Nafey, M. Abdelkader, A. Abdelmotalip, A.A. Mabrouk, Parameters affecting solar still productivity, Energy Convers. Manag. 41 (2000) 1797–1809, https://doi.org/10.1016/S0196-8904(99)00188-0.
[51] R. Tripathi, G.N. Tiwari, Effect of Water Depth on Intemal Heat and Mass Transfer for Active Solar Distillation, vol. 173, 2005, pp. 187–200, https://doi.org/10.1016/j.desal.2004.08.03.
[52] M.K. Phadatare, S.K. Verma, Influence of Water Depth on Internal Heat and Mass Transfer in a Plastic Solar Still, vol. 217, 2007, pp. 267–275, https://doi.org/10.1016/j.desal.2007.03.006.
[53] A.A. El-Sebaii, Effect of Wind Speed on Active and Passive Solar Stills, vol. 45, 2004, pp. 1187–1204, https://doi.org/10.1016/j.enconman.2003.09.036.
[54] A.Y. Hashim, J.M. Al-asadi, W.A. Taha, Experimental Investigation of Symmetrical Double Slope Single Basin Solar Stills Productivity with Different Insulation, 2009, p. 1.
[55] L. An, C. Liu, Y. Liu, Optimization of operating parameters in polysilicon chemical vapor deposition reactor with response surface methodology, J. Cryst. Growth (2018), https://doi.org/10.1016/j.jcrysgro.2018.02.030.
[56] I. George, R. Kalaivanan, Optimization of thermal performance on evacuated tube solar collector water heating, System 7 (2017) 47–55, https://doi.org/10.9790/9622-0710074755.
[57] T.B. Gorji, A.A. Ranjbar, Geometry optimization of a nanofluid-based direct absorption solar collector using response surface methodology, Sol. Energy 122 (2015) 314–325, https://doi.org/10.1016/j.solener.2015.09.007.
[58] G. Naja, B. Ghobadian, T. Yusaf, S. Mohammad, R. Mamat, Optimization of performance and exhaust emission parameters of a SI (spark ignition) engine with gasoline e ethanol blended fuels using response surface methodology, 2015, https://doi.org/10.1016/j.energy.2015.07.004.
[59] M. Hatami, D. Jing, Optimization of wavy direct absorber solar collector (WDASC) using, Appl. Therm. Eng. (2017), https://doi.org/10.1016/j.applthermaleng.2017.04.137.
[60] M.S. Yousef, H. Hassan, M. Ahmed, S. Ookawara, Energy and exergy analysis of single slope passive solar still under Egyptian climate conditions, Energy Procedia 141 (2017) 18–23, https://doi.org/10.1016/j.egypro.2017.11.005.